Converging evidence that left extrastriate body area supports visual sensitivity to social interactions

Marco Gandolfo[1*], Etienne Abassi[4*], Eva Balgova[2,3], Paul E. Downing[2], Liuba Papeo[4], Kami Koldewyn[2]

1. Donders Institute, Radboud University, Nijmegen, NL.
2. Department of Psychology, Bangor University, Gwynedd, UK
3. Department of Psychology, Aberystwyth University, Aberystwyth, Ceredigion, UK
4. Institut des Sciences Cognitives, Marc Jeannerod, Lyon, France

*Joint first authors

Corresponding authors:
Marco Gandolfo marco.gandolfo@donders.ru.nl
Address: Thomas van Aquinostraat 4, 6525GD, Nijmegen, The Netherlands

Kami Koldewyn k.koldewyn@bangor.ac.uk
Address: Brigantia building, LL572AS, Bangor, UK

Abstract

Navigating our complex social world requires processing the interactions we observe. Recent psychophysical and neuroimaging studies provide parallel evidence that the human visual system may be attuned to efficiently perceive dyadic interactions. This work implies, but has not yet demonstrated, that activity in body-selective cortical regions causally supports efficient visual perception of interactions. We adopt a multi-method approach to close this important gap. First, using a large fMRI dataset (N=92), we found that the left-hemisphere Extrastriate Body Area (EBA) responds more to face-to-face than non-facing dyads. Second, we replicated a behavioural marker of visual sensitivity to interactions: categorisation of facing dyads is more impaired by inversion than non-facing dyads. Third, we used fMRI-guided transcranial magnetic stimulation to show that online stimulation of the left EBA, but not a nearby control region, abolishes this selective inversion effect. Activity in left EBA, thus, causally supports the efficient perception of social interactions.

Introduction

As a social species, humans are constantly engaged in interactions with each other. This places strong demands on neural systems that must make sense of others' behaviour and attempt to infer underlying emotional and mental states as well as discern longstanding traits (Adolphs, 2001, 2009; Brothers, 1990). While we stand to learn much from our own direct interactions with others, many valuable social cues are also found in observing the interactions between other individuals. Such observed interactions can carry unique cues about others' relationships, social skills, goals, and personalities. Accordingly, in contrast to much of the "social vision" work on perception of social cues from individual faces, bodies, and voices (Adams et al., 2011; Belin et al., 2011; Duchaine & Yovel, 2015; Hu et al., 2020; Peelen & Downing, 2007), researchers have recently turned their attention to the visual processes underpinning perception of interactions per se. One recent perspective is that facing pairs (dyads) of humans elicits an emergent, holistic percept, one that is more than the sum of its component parts, and that may engage unique perceptual processes. This proposal has been supported, for example, by findings that facing dyads are more readily detected in a visual search task (Papeo et al., 2019), and that they are particularly prone to the disrupting effects of in-plane inversion (Papeo, 2020; Papeo et al., 2017), a trait they have in common with individual faces (Yin, 1969) and bodies (Gandolfo & Downing, 2020; Griffin & Oswald, 2022; Reed et al., 2003).

Indeed, just as the face inversion effect is thought to be a marker of the holistic processing of faces (Maurer et al., 2002; Rezlescu et al., 2017; see also Gerlach & Mogensen, 2023), the increased inversion effect elicited by facing *versus* non-facing dyads (Abassi & Papeo, 2022; Papeo, 2020; Papeo et al., 2017) may indicate that facing dyads – like faces – are processed holistically. This has a few important implications. First, it suggests that individuals in facing dyads are bound together perceptually and processed as a unit, in a manner that is more similar to the processing of single bodies or faces than to independent perceptual objects. Second, it suggests that humans have a visual specialisation for facing dyads, which may function as a basic 'template' that perceptually highlights social interactions. Thus, the two-body inversion effect (from here, "2BIE": the stronger inversion effect for facing vs. non-facing bodies) may be a behavioural marker for the first stage of social interaction perception and processing. That is, visual specialisation for the specific configuration formed by facing dyads may allow for the quick detection of social interactions in the world. One advantage of such a basic perceptual pattern is that this would facilitate attention to social interactions, supporting more efficient cognitive analysis of the observed interaction.

What are the brain mechanisms supporting this proposed visual specialisation for social interactions? Recent studies have generated new neuroscientific evidence about the perception of interacting dyads. Studies focused on *dynamic* interactions (Isik et al., 2017; Lee Masson & Isik, 2021; Walbrin et al., 2018) have highlighted a region of the posterior superior temporal sulcus (pSTS) as being selectively involved in the perception of observed social interactions, including interactions depicted by full-cue movies (e.g. Landsiedel et al., 2022) animated shapes (Castelli et al., 2000; Walbrin et al., 2018), point-light animations (Centelles et al., 2011; Sapey-Triomphe et al., 2017; Walbrin et al., 2018), and animated mannikins (Georgescu et al., 2014). This region, however, does not respond to *static* depictions of interactions (Landsiedel et al., 2022), including the kind of "prototypical" facing

dyads that so reliably produce the 2BIE. As such, it is unlikely that the pSTS is centrally involved in the early stages of social interaction detection as described above.

Indeed, other recent neuroimaging evidence implicates more posterior occipitotemporal regions in the perception of interacting dyads, even in a static format. In particular, several studies have suggested the relevance of the “extrastriate body area” (EBA; (Downing et al., 2001) in perception of both static and dynamic dyads. To date, most of the research on the functional properties (Downing & Peelen, 2011) and causal relevance (Downing & Peelen, 2016) of this region for social vision has focused on the perception of individual bodies or parts of the body. But recent studies using static images of dyads who are either facing each other as if interacting, or not, have suggested that the EBA is uniquely engaged by facing human dyads (Abassi & Papeo, 2020, 2022). Importantly, work investigating which regions of the brain are most involved in the detection of facing dyads, and the two-body inversion effect, suggests that the size of the 2BIE is directly and specifically related to activity in the EBA (Abassi & Papeo, 2022).

To date, however, evidence for the contribution of EBA to interaction perception remains correlational, and limited to single fMRI studies. Important causal evidence about the functional roles of regions in the lateral occipitotemporal cortex (LOTC) in visual processing of single items such as faces, bodies, or objects has come from transcranial magnetic stimulation (TMS) studies (Pitcher et al., 2009). With online TMS, for example, the contribution of category selective regions including the occipital face area (Pitcher et al., 2007), the lateral occipital complex (Dilks et al., 2013; Wischnewski & Peelen, 2021), and EBA (Gandolfo & Downing, 2019; Urgesi et al., 2004; van Koningsbruggen et al., 2013), has been explored. These studies show that TMS selectively impairs performance of tasks requiring attention to images of people or objects in a region- and task-specific manner (Pitcher et al., 2008). Accordingly, they suggest the possibility that a similar interference approach may test hypotheses about the causal contribution of targeted brain areas to interaction perception.

In the current study (see **Figure 1**), we first provide solid correlational evidence for a contribution of the occipito-temporal cortex in interaction perception via a re-analysis of a large neuroimaging dataset. Consistently across participants, results show strong selectivity in the left EBA for visual perception of facing dyads. We then demonstrate the specific and causal role of this region in such functional specialization, using fMRI-guided brain stimulation. In particular, we applied online TMS to the left EBA (localised individually with fMRI) while participants performed a categorization task to measure the 2BIE. The typical pattern of performance in this task, taken as a marker of the visual functional specialization for facing bodies (Papeo et al., 2017; Papeo & Abassi, 2019), is that the effect of inversion on object recognition is more severe for facing than for non-facing dyads, and this does not generalise to control non-body objects (chairs). We replicated the 2BIE in a new sample of participants, and then showed that this facing-direction and category-specific inversion effect was effectively eliminated with online application of TMS over left EBA. In sum, with this rich set of results, we highlight a previously uncharted visual processing stage in social interaction perception and connect it mechanistically to functional specialization in the human visual cortex.

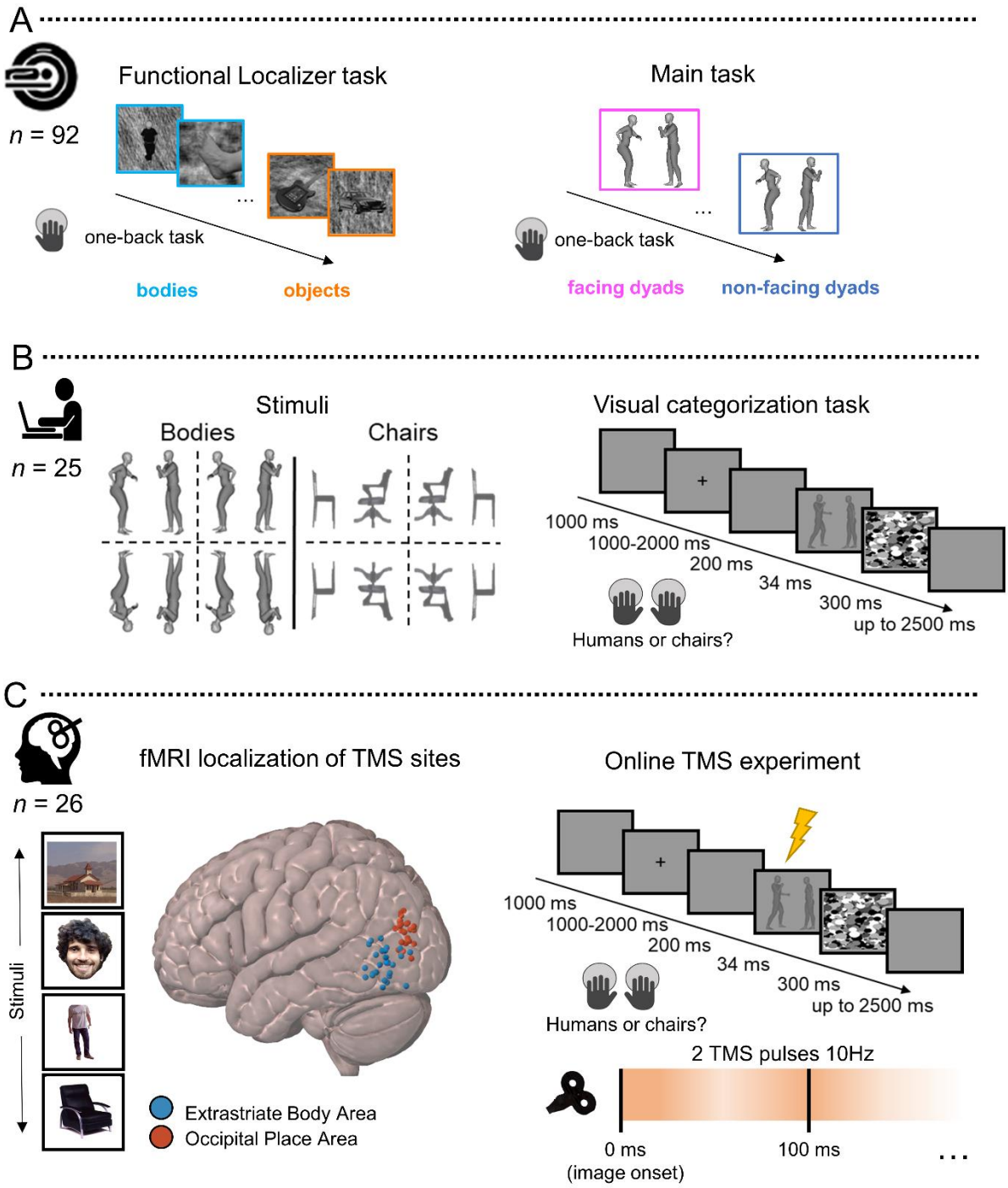

Figure 1. *Workflow and schematic display of the procedure across the three experiments. The multi-method approach includes correlational and causal neuroscientific methods. As such, it allows us to directly link brain activity in focal regions with behavioural outcomes.* **A.** *fMRI study. Left: Examples of stimuli used in the functional localiser task. Extrastriate body area (EBA) was localised with the contrast: bodies > [faces, places, & objects]; Occipital place area (OPA) was localised with the contrast places > [faces, bodies, & objects]. Right: Example of stimuli for key fMRI contrast: facing > non-facing dyads; main experimental task.* **B.** *Behaviour-only experiment. Left: Examples of experimental stimuli. On each trial, a pair of bodies or chairs were shown upright or inverted, and either facing toward or away from each other. Right: Visual categorization task structure and trial procedure to measure the two-body inversion effect (2BIE).* **C.** *fMRI-localisation guided TMS experiment. Left: stimuli from the localiser task (the face illustrated was not presented in the real*

*experiment, and is the face of the Author (MG)). The localiser session outcomes are displayed on a 3D MNI brain template as normalised individual stimulation site coordinates for the EBA (in blue) and the OPA (in red) for each participant (see also **Figure S7**). Bottom: the rTMS session procedure and parameters.*

Results

Interacting human dyads preferentially engage the left EBA: fMRI evidence

We first performed a new whole-brain fMRI analysis by combining data from 92 participants in three independent fMRI studies (Abassi & Papeo, 2020, 2022, 2023). In each of these studies, participants saw the same critical conditions (facing and non-facing body dyads, Figure 1A). We used a random-effects general linear model (RFX GLM) to estimate the effect of the facing direction between bodies in a dyad with the contrast facing > non-facing body dyads. Using a voxelwise threshold of $p \leq 0.05$, corrected for multiple comparisons using familywise error (FWE) at the voxel level, this contrast (Figure 2a) showed an effect in a bilateral cluster within the LOTC peaking in the middle occipital gyrus for the left hemisphere and in the middle temporal gyrus for the right hemisphere. Comparison with the results of a blocked-design functional localizer experiment revealed considerable overlap of this cluster with the EBA at the group-average level. The cluster in the left hemisphere was larger than the cluster in the right hemisphere (Left: 354 voxels, peak MNI coordinates: -52, -76, 12, peak z = 6.26; Right: 14 voxels, peak MNI coordinates: 48, -66, 6, peak z = 4.97, **Figure 2A**). To assess for a significant difference of the overall level of activity between these two clusters, we performed regions of interest (ROI) analyses as follows.

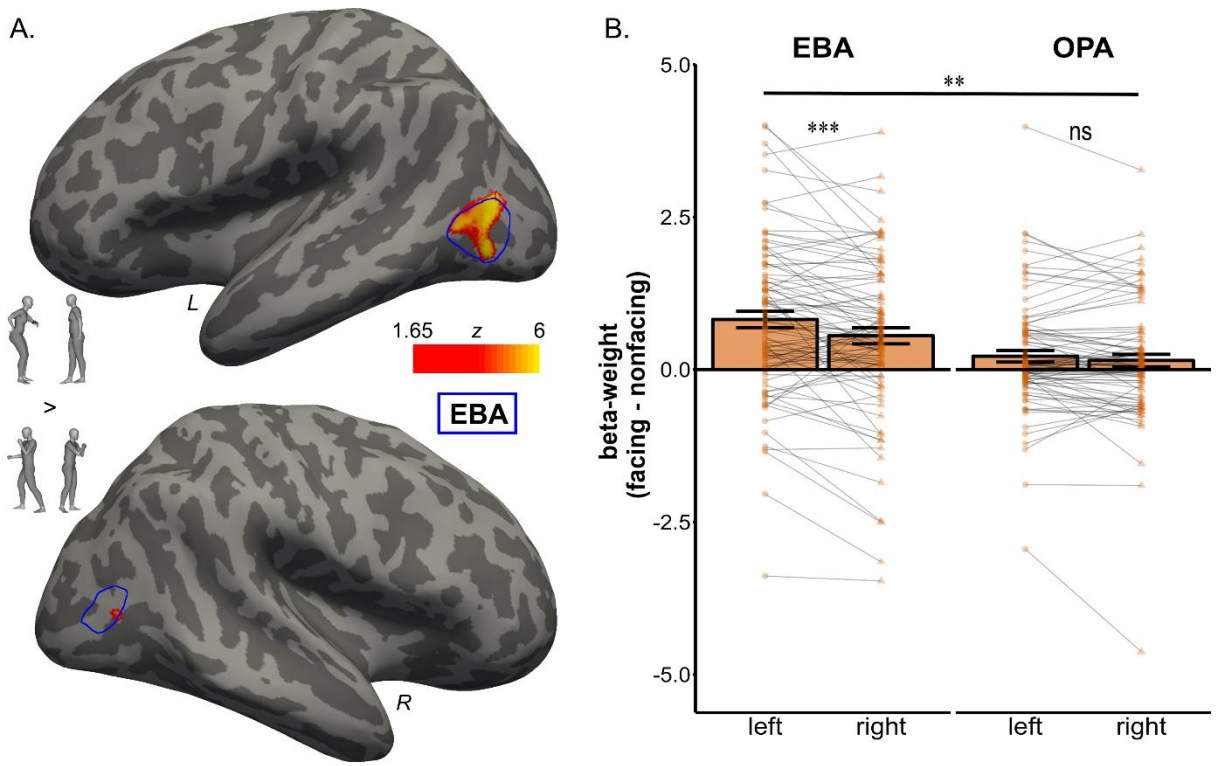

Figure 2. *Comparison of brain activity between facing and non-facing dyads.* **A.** *Univariate second-level (group) analysis for the whole-brain contrast facing > non-facing (N = 92). Voxelwise threshold of p ≤ 0.05, FWE corrected at the voxel level. The EBA highlighted in blue corresponds to the results of the group-level random-effect contrasts of bodies > [objects+faces+places].* **B.** *ROI analysis. The bar chart shows the facing > nonfacing effect in the EBA and OPA for the left and the right hemisphere. Left hemispheric activity shows a significantly larger difference between the two conditions in the EBA only.*

Using data from the functional localizer task, for each participant we identified two ROIs, separately for each hemisphere: the EBA by taking the 200 voxels with the highest selectivity for body-stimuli within an anatomical mask of the middle occipitotemporal cortex, and the OPA by taking the 200 voxels with the highest selectivity for scene-stimuli within the same anatomical mask. To measure the lateralization of the effect of viewing a facing dyad as compared to a non-facing dyad, for each ROI we directly compared the mean neural activity over participants, for facing and non-facing dyads within each hemisphere. A repeated-measures ANOVA with three factors, ROI (EBA/OPA), hemisphere (Left/Right), and facing direction (facing / non-facing), showed a significant three-way interaction ($F(1,91) = 7.36$; $p = 0.008$; $\eta_p^2 = 0.07$, **Figure 2B**). Within the EBA-ROI, we found a significant hemisphere by facing direction interaction ($F(1,91) = 13.71$; $p < 0.001$; $\eta_p^2 = 0.13$). There was a larger difference in neural response between facing and non-facing dyads in the left EBA ($t(91) = 6.20$, $p < 0.001$, d = 0.65, 95% CI [0.44, 0.85], $BF_{10} = 696000$, Mean difference = 0.82, SE = 0.11), than in the right EBA ($t(91) = 4.19$, $p < 0.001$, d = 0.44, 95% CI [0.23, 0.64], $BF_{10} = 281$, Mean difference = 0.55, SE = 0.11, see Figure 2b). In contrast, in our control OPA-ROI, we did not observe a significant hemisphere by facing direction interaction ($F(1,91) = 2.41$; $p = 0.124$; $\eta_p^2 = 0.03$, $BF_{10} = 0.37$). These findings together confirm that the facing direction effect was specific to the EBA, and preferentially lateralized to the left hemisphere.

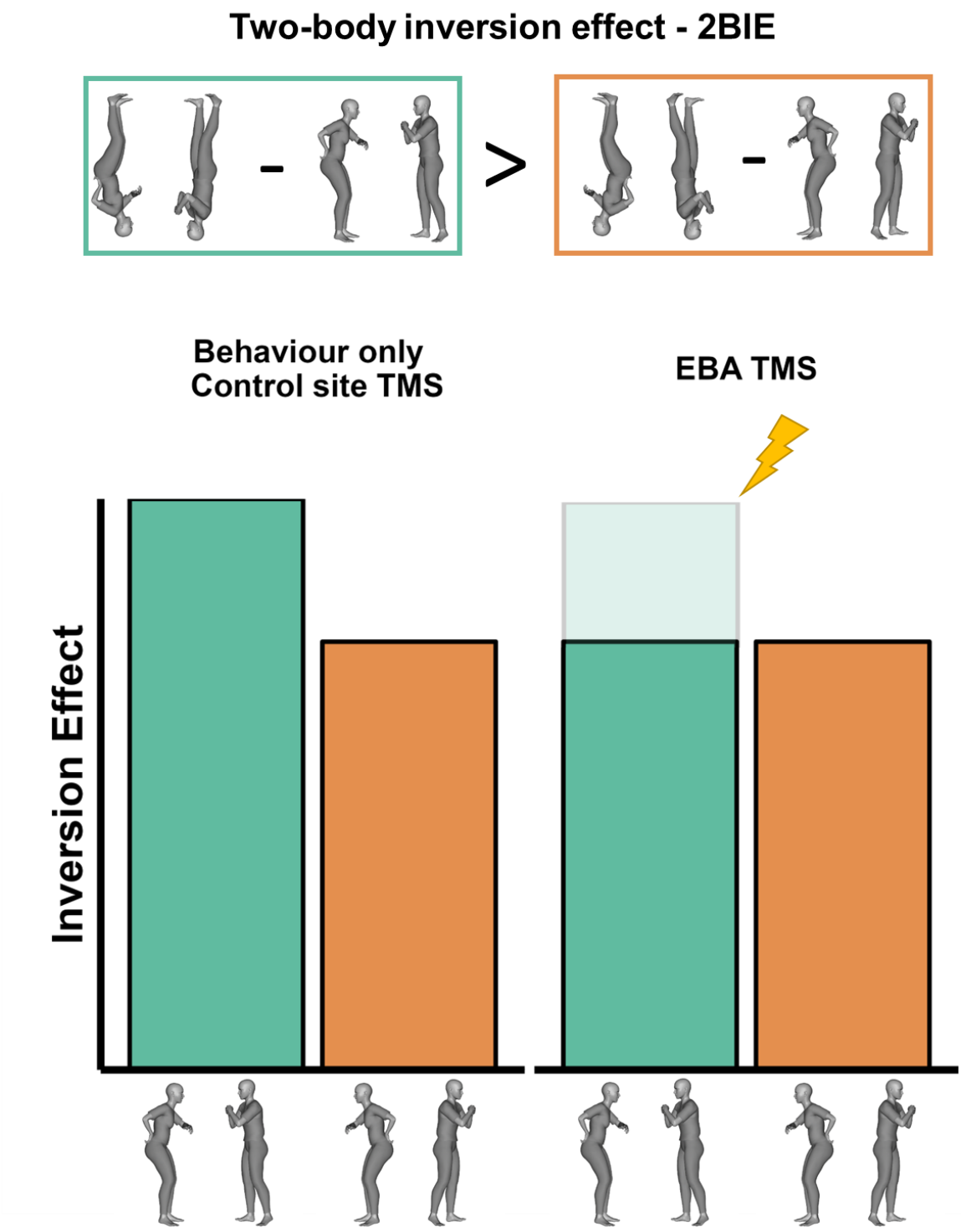

Figure 3. *The 2BIE (two-body inversion effect) is taken as a behavioural marker for first-stage social interaction processing. This is measured as increased inversion effects (i.e. difference in performance between inverted and upright body categorization) for facing vs. non-facing dyads. Here, we show the expected pattern of results on the 2BIE for the fMRI*

guided TMS experiment. EBA stimulation is expected to selectively disrupt the 2BIE while effect should remaining intact (i.e., similar to the 2BIE measured in a behaviour only task) after stimulation of the control site (i.e. the OPA).

The behavioural two body inversion effect (2BIE)

Our next step was to test the hypothesis that the left EBA is causally necessary for the processing of facing human dyads (**Figure 3**). To do so, we first replicated the 2BIE (Papeo et al., 2017). Participants performed a categorisation task to discriminate briefly-presented images of people *vs* chairs (**Figure 1B**). Each image contained two items (people or chairs) that were facing toward or away from each other, and orthogonally either upright or inverted. The 2BIE occurs when the facing human dyads show larger inversion effects – measured by an increase in errors -- than their non-facing counterpart (**Figure 3**). In contrast, in line with prior findings, we did not expect to see similar effects for the control objects (chairs).

As predicted, we observed a greater inversion effect for facing dyads than for non-facing dyads, as revealed by a significant three-way interaction among Stimulus (bodies, chairs), Orientation (upright, inverted), and Facing direction (facing, non-facing), $F(1,22) = 9.11$, $p = 0.006$, $\eta_p^2 = 0.29$. For human stimuli, the inversion effect for facing dyads was larger than for the non-facing dyads (**Figure 4A**, $t(22) = 3.014$, $p = 0.006$, d = 0.63, 95% CI [0.02, 0.12], $BF_{10} = 7.16$, Mean Difference = 0.07, SE = 0.02). This difference was absent when comparing the inversion effect for facing and non-facing chairs (**Figure S3**) ($t(22) = -0.40$, $p = 0.696$, d = -0.08, 95% CI [-0.03, 0.02], $BF_{10} = 0.24$, Mean Difference = -0.01, SE = 0.01; See supplemental materials). We take this facing-direction and category-specific inversion effect as the behavioural marker of early-stage visual processing of social interaction that we then targeted in the subsequent neurostimulation study.

Left-EBA is causally necessary for encoding facing human dyads

If activity of the left hemisphere EBA directly contributes to early-stage processing of static social interactions, as indicated by our correlational evidence from fMRI, then online stimulation of this region should selectively disrupt the 2BIE (**Figure 3**). Further, this TMS effect should be category-specific (only occurring with human dyads) and site-specific (only occurring after left EBA stimulation). Note that these hypotheses were pre-registered (https://aspredicted.org/4CZ_GGG).

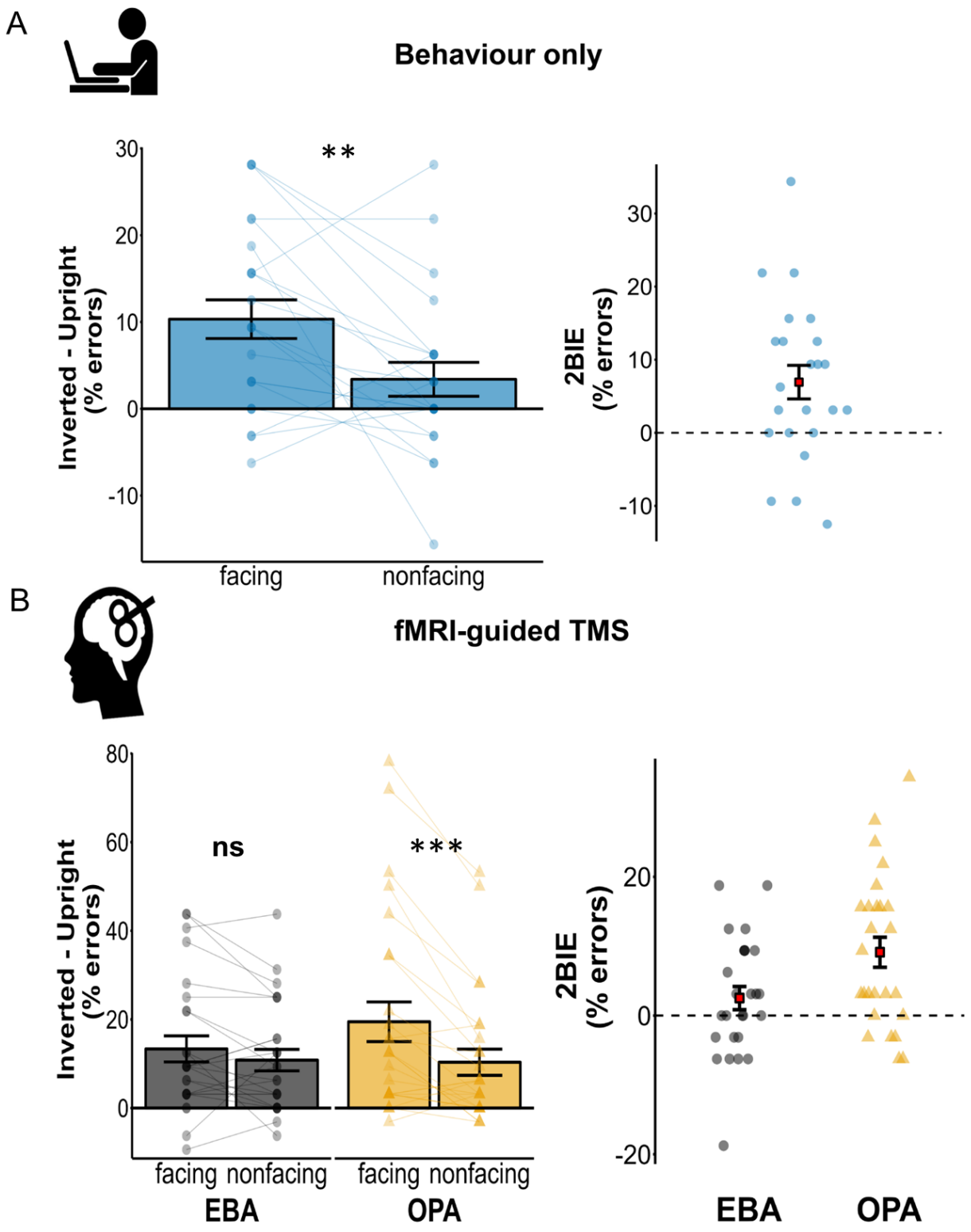

Figure 4. A. *Behaviour-only experiment (N = 25). The left panel bar chart shows the inversion effect (% of errors in the inverted – upright trials) for human dyad stimuli in the facing vs non-facing condition. The right panel illustrates the 2BIE, expressed as the subtraction of the inversion effect for non-facing dyads from that for facing dyads.* ***B.*** *fMRI guided TMS-experiment (N = 26). The left panel shows the inversion effect (% of errors in*

the inverted – upright trials) for human dyad stimuli in the facing vs non-facing condition for both the EBA (site of interest) and the OPA (control TMS site). The right panel shows the 2BIE (inversion effect for facing – inversion effect for non-facing dyads) during EBA vs OPA stimulation. TMS on the EBA reduced the 2BIE; TMS on the OPA (control site) yielded a pattern of results consistent with that seen in the behaviour-only experiment (note that the behaviour-only and fMRI-guided TMS experiment were conducted with different participants). The full barchart including all of the condition means can be found in ***Figure S1.*** *Lines and datapoints indicate individual participant's means in the respective conditions. Error bars indicate the standard error of the mean. * p < .05; ** p < .01; *** p < .005.*

As predicted, we found that left EBA stimulation selectively eliminated the 2BIE, and therefore the TMS effects on the categorization task were category- and site-specific (**Figure 4B**). This was revealed by a significant site (EBA, OPA) x stimulus (body, chair) x orientation (upright, inverted) x facing-direction (facing, non-facing) interaction, $F(1,25) = 4.92$, $p = 0.036$, $\eta_p^2 = 0.16$.

To clarify the nature of this interaction, we conducted separate three-way ANOVAs for each region of interest. When TMS was applied to the control site OPA, the selective effect of inversion on facing dyads was confirmed, similar to the 2BIE found without TMS (behaviour-only experiment), as evidenced by a Stimulus x Orientation x Facing-direction interaction ($F(1,25) = 9.90$, $p = 0.004$, $\eta_p^2 = 0.28$, $BF_{10} = 9.79$). In contrast, when TMS was applied to EBA the interaction that characterizes the 2BIE was not significant ($F(1,25) = 0.31$, $p = 0.581$, $\eta_p^2 = 0.01$). Further, a Bayesian analysis of this contrast indicated positive evidence for the null hypothesis ($BF_{10} = 0.24$).

Indeed, when directly comparing the effect of stimulation at the two stimulation sites when participants were viewing dyads of people, we found a site x orientation x facing-direction interaction ($F(1,25) = 9.87$, $p = 0.004$, $\eta_p^2 = 0.28$). That is, the inversion effect for the facing human dyads was larger than for their non-facing counterpart after left OPA stimulation ($t(25) = 4.22$, $p < 0.001$, $d = 0.83$, 95% CI [0.05, 0.14], $BF_{10} = 105.79$, Mean Difference = 0.09, SE = 0.02). In contrast, those conditions did not reliably differ after left EBA stimulation ($t(25) = 1.51$, $p = 0.144$, $d = 0.30$, 95% CI [-0.01, 0.06], $BF_{10} = 0.57$, Mean Difference = 0.03, SE = 0.02).

Finally, no difference between facing and non-facing orientation was found for the control chair stimuli ($F(1,25) = 0.62$, $p = 0.438$, $\eta_p^2 = 0.02$, **Figure S2**) demonstrating that neither left EBA ($t(25) = 0.39$, $p = 0.702$, $d = 0.08$, 95% CI [-0.04, 0.06], $BF_{10} = 0.22$, Mean Difference = 0.01, SE = 0.03) nor left OPA ($t(25) = -0.86$, $p = 0.397$, $d = 0.28$, 95% CI [-0.07, 0.03], $BF_{10} = 0.29$, Mean Difference = -0.02, SE = 0.02) stimulation affected performance in this condition. Together, these analyses confirm that the effects of TMS on the 2BIE were both site and category specific, as predicted.

General Discussion

Here, we present the first causal evidence for the contribution of occipitotemporal social perception regions, specifically left EBA, to the perception of interacting (face-to-face) human dyads. First, we demonstrate across a large group of participants that left EBA, in particular, is more responsive to facing dyads than non-facing dyads. We then demonstrate that TMS to left EBA effectively eliminates the two-body inversion effect, which is proposed to constitute a signature of early processes in social interaction perception. The specificity of this result to human stimuli (*vs* chairs) demonstrates that it is not due to a generic disruption of visual processing. The specificity of this result to left EBA stimulation (*vs* nearby OPA) demonstrates that reduction of the 2BIE does not necessarily follow disruption of any given occipitotemporal region, nor is it due to non-specific 'annoyance' caused by TMS, such as task interference due to stimulator noise, or discomfort caused by TMS pulses (see Meteyard & Holmes, 2018).

We identify two possible interpretations of our results that further specify the nature of the causal contribution made by left EBA to perceiving dyadic interactions. First, the two-body inversion effect is thought to relate to holistic processing of prototypical human face-to-face interactions when dyads are seen in their canonical upright orientation (Papeo et al., 2017). Thus, left EBA activity may normally capture an emergent property of interacting dyads that reflects their status as a "unit" of visual processing (Adibpour et al., 2021), beyond its response to individual bodies. This idea is in line with previously observed sensitivity for other kinds of typically-observed object configurations in the LOTC (Kaiser et al., 2019; Kaiser & Peelen, 2018; Papeo, 2020).

Second, the TMS effect we report here could also be a result of the disruption of EBA's contribution to the perception of individual body postures. Specifically, TMS to EBA may reduce the facing-specific inversion effect by disrupting the body posture signals that would normally help distinguish facing from non-facing pairs. This contribution of EBA to body posture may be particularly strong for inverted postures: if inversion disrupts whole-body representations, then encoding of the body posture must rely more on part-based body representations. Indeed, previous evidence from fMRI (Taylor et al., 2007; Taylor & Downing, 2011) indicates an emphasis on body-part representations in EBA, relative, for example, to whole-body representations in the fusiform body area (FBA; Peelen & Downing, 2005; Schwarzlose et al., 2005). Relatedly, Urgesi et al. (2007) found that TMS stimulation of EBA was particularly disruptive for judgments of single inverted bodies, relative to upright ones. This account would also predict a general disruption of the inversion effect for pairs of bodies in the present study, regardless of facing direction. However, this pattern was not clearly demonstrated in our data (i.e., the stimulus x orientation x site interaction was not significant). Likewise, it does not easily account for the increased response to facing over non-facing dyads in EBA in our, and others, fMRI data. Future work will be necessary to test the extent to which TMS disruption of part-based body processing contributes to the effect we report here. Importantly, these two explanations proposed here are not mutually exclusive. Indeed, EBA's sensitivity to single-body posture information may also be instrumental in its representation of dyadic interactions holistically.

Our demonstration of a relatively greater fMRI response to static interacting dyads in left rather than right hemisphere EBA contrasts with a general tendency for the effects of social

stimuli (people and their movements) on visual cortex activity to be relatively right-hemisphere lateralised (Allison et al., 1999; Downing et al., 2001; Isik et al., 2017; Kanwisher et al., 1997; etc.). More generally, evidence from neuropsychological studies suggests a relatively greater involvement of the right hemisphere in holistic or global perception and, in contrast, an emphasis on parts or local processes in the left hemisphere (e.g., Robertson, 1995). How to reconcile our findings with these established patterns? One intuitive possibility is that our result could be related to the left-lateralised hand-selective region that is near to, but distinct from, EBA (e.g. Bracci et al., 2010). When we observe dyadic interactions in the world, people are more likely to be reaching towards than away from each other. When presenting those stimuli in the lab, extremities (hands, feet) are thus more likely to appear on or near the fovea in facing than in non-facing dyads, which could drive hand-selective regions more strongly for facing dyads. This is not, however, the case for our stimuli, where the distance between the nearest point (usually hands or feet) and the screen centre was matched between facing and non-facing dyads, across stimuli. In addition, the distance between hands and/or feet is *exactly* the same for inverted dyads as for upright dyads. Thus, a strong visual representation of the hands in the left hemisphere would not in itself account for the present fMRI or TMS results. Instead, we propose a related possibility, that sensitivity to social interactions in left EBA is related to findings that many aspects of actions are represented in the wider lateral occipitotemporal cortex, and particularly so in the left hemisphere (Lingnau & Downing, 2015). Our fMRI results may reflect the increased processing needed to represent body and limb postures that predict interaction-specific actions when dyads face each other. Thus, our results are not necessarily in conflict with what we already know about EBA, but instead may show a complementary functional specialisation in left EBA for representing body information relevant to predicting joint (interactive) actions.

Here, we have focused on the role of EBA in interaction perception. Prior work suggests that both EBA and pSTS are sensitive to visual cues to dyadic interaction, including facing direction. However, pSTS appears to only be sensitive to such interactive cues when they are presented dynamically (Landsiedel et al., 2022), while EBA shows sensitivity to dyadic facing direction for both static and dynamic stimuli (Abassi & Papeo, 2020; Bellot et al., 2021; Landsiedel et al., 2022; Walbrin & Koldewyn, 2019). Additionally, at least for dynamic social stimuli, visual information is proposed to feed from EBA to pSTS (Giese & Poggio, 2003; Pitcher & Ungerleider, 2021). Indeed, recent evidence shows that functional connectivity between EBA and pSTS is increased during the perception of dyads that move towards vs away from each other (Bellot et al., 2021). Thus, the two regions likely work together during ‘real world’ perception of social interactions. This proposal prompts a wealth of future research questions. Is motion necessary for information flow between EBA and pSTS? What, specifically, does pSTS add to the processing of social interactions? How does information flow beyond EBA and pSTS to support higher-level social cognitive processes, social inferences, and social judgements?

Concluding remarks:

Using a multimodal approach, we demonstrate that left EBA is not only sensitive to interactive information but is causally necessary for the efficient perception of facing dyads. Rapid detection of dyads may reflect a processing stage that is critical for recognising and understanding social interactions in a cluttered visual world. As such, our results strongly support the idea that understanding social interactions is underpinned by basic visual

processes, critically relying on discriminating between interacting and non-interacting human groups. Importantly, although future work is needed to fully explore the role EBA plays in social interaction perception and social inference, our results also demonstrate a novel functional specialisation in left EBA.

Methods

fMRI experiments

Participants: fMRI. We combined data from 92 unique participants (52 females; mean age 24.8 years, SD = 3.7) included in one of three previous independent fMRI studies (*N* 20 from Abassi and Papeo, 2020; *N* 30 from Abassi & Papeo, 2022; *N* 42 from Abassi & Papeo, 2023). All participants had normal or corrected-to-normal vision, reported no history of psychiatric or neurological disorders, or use of psychoactive medications. They were screened for contraindications to fMRI and gave written informed consent. All studies were approved by the local ethics committee (CPP Sud Est V, CHU de Grenoble).

fMRI Stimuli. In all three studies, stimuli were created from grayscale renderings of human bodies in various biomechanically possible poses, in a profile view, arranged in pairs, to form face-to-face (facing) dyads or back-to-back (non-facing) dyads. Non-facing body dyads were created by swapping the position of the two bodies in each facing body dyad. Distance between the two bodies in a dyad was matched across facing and non-facign dyads so that the two sets only differed for the relative positioning of the bodies. We used Daz3D (Daz Productions, Salt Lake City) and the Image Processing Toolbox of MATLAB (The MathWorks Inc, Natick, Massachusetts) to create and edit stimuli. For a full description of the stimuli, we refer the reader to Abassi & Papeo (2020; 2022; 2023).

Inside the scanner, a liquid crystal projector (frame rate: 60 Hz; screen resolution: 1024 × 768 pixels, screen size: 40 x 30 cm) was used to back-project the stimuli onto a screen. Participants viewed the stimuli binocularly (~7° of visual angle) through a mirror above the head coil. Stimulus presentation, response collection, and synchronization with the scanner were controlled with Psychtoolbox (Brainard, 1997) through MATLAB (MathWorks).

fMRI data acquisition. Imaging in all three studies was conducted on the same MRI machine, a MAGNETOM Prisma 3T scanner (Siemens Healthcare) at the CERMEP imaging centre in Bron (France). T2*-weighted functional volumes were acquired using a gradient-echo echo-planar imaging sequence with slightly different values across studies due to the fact in studies 2 and 3 multiband acquisitions were employed (Study 1: GRE-EPI; TR/TE = 2200/30 ms, flip angle = 90°, acquisition matrix = 74x74, 40 slices, FOV= 220x220 mm, 40 slices, slice thickness = 3 mm, no gap, acceleration factor = 2 with GRAPPA reconstruction and phase encoding set to anterior/posterior direction; Study 2-3: GRE-EPI; TR/TE = 2000/30 ms, flip angle = 80°, acquisition matrix = 96x92, FOV = 210x201 mm, 56 slices, slice thickness = 2.2mm, no gap, multiband acceleration factor = 2 and phase encoding set to anterior/posterior direction). For all studies, acquisition of high-resolution T1-weighted anatomical images was performed in the middle of the main experiment and lasted 8 min (MPRAGE; TR/TE/TI = 3000/3.7/1100 ms, flip angle = 8°, acquisition matrix = 320x280, FOV = 256x224 mm, slice thickness = 0.8mm, 224 sagittal slices, GRAPPA accelerator factor = 2). Acquisition of two field maps was performed at the beginning of each fMRI session.

fMRI task procedure. All studies included three runs featuring blocks of upright facing or non-facing dyads (randomized with other type of runs that varied across study). The structure of blocks was identical across studies, although with slight variation in the duration of events. Each block included 5-to-8 stimuli of the same condition (facing or non-facing) presented for 400-to-550 ms, interleaved with a black central fixation cross, which changed color (from black to red) in 37.5% of all stimulation and fixation trials. Participants were instructed to fixate the cross throughout the experiment and detect and report the color change by pressing a button with their right index finger. This task was used to minimize eye movements and maintain vigilance in the scanner. For more information on the specificities of each study, we refer the reader to Abassi & Papeo (2020; 2022; 2023).

Functional localizer tasks. For all studies, in addition to the experimental runs, subjects completed a functional localizer task of 2-to-3 runs, with stimuli and task adapted from the fLoc package (Stigliani et al., 2015). In all three studies, the functional localizer task included grayscale photographs of: 1) bodies; 2) faces; 3) places; and 4) inanimate objects. Within a run, the duration of each block was four seconds, with 12 blocks for each object class over the run and eight images per block (500 ms per image without interruption), randomly interleaved with 12 baseline blocks (empty screen).

Preprocessing of fMRI data. Functional images were pre-processed and analysed using SPM12 (Friston et al., 2007) as implemented in MATLAB. The first four volumes of each run were discarded, taking into account initial scanner gradient stabilization (Soares et al., 2016). The pre-processing of the remaining volumes involved de-spiking, slice time correction, geometric distortion correction using field maps, spatial realignment and motion correction using the first volume of each run as reference. Anatomical volumes were co-registered to the mean functional image, segmented into grey matter, white matter and cerebrospinal fluid, and aligned to the Montreal Neurological Institute (MNI) template. To normalise the functional images, we used the DARTEL method (Ashburner, 2007) to create flow fields for each subject and an inter-subject template, registered in the MNI space. Finally, the voxels were resampled to $2mm^3$, spatially smoothed with a Gaussian kernel of 6 mm FWHM and low-frequency drifts were removed with a temporal high-pass filter (cutoff 128 s).

Whole-brain univariate analyses. Random-effects general linear model (RFX GLM) analyses were conducted to estimate the blood-oxygen-level-dependent (BOLD) signal. The model comprised two regressors for the experimental conditions (facing and non-facing dyads), one regressor for the fixation blocks, and six nuisance regressors for movement correction parameters. The facing > non-facing effect in the second-level (group) analysis was determined using a voxelwise threshold of $p \leq 0.05$ which was family wise error (FWE) corrected at the voxel level to correct for multiple comparisons.

Definition of regions of interest (ROIs). For each subject, using data from the functional localiser task, we identified voxels showing the highest response to bodies in the bilateral EBA using the contrast bodies > faces+objects+places, and to places in the bilateral OPA, using the contrast places > faces+objects+bodies. Individual subject localiser data were entered into a GLM with one regressor for each object-class condition (bodies, places, faces and objects), one for baseline blocks, and six nuisance regressors for movement correction parameters. One mask of the left and one of the right middle occipitotemporal cortex was created using FSLeyes (McCarthy, 2018) and the Harvard-Oxford Atlas (Desikan et al.,

2006) implemented in FSL (Jenkinson et al., 2012). For each participant, within this mask, we first selected the voxels with significant activation (threshold: p = 0.05) for each of the above two contrasts. For each individual, the two final ROIs included up to the 200 voxels with the highest t-values.

ROIs analyses. The mean activation estimation parameters for facing and non-facing dyads were extracted and analyzed in a 2 ROI (EBA/OPA) x 2 hemispheres (left / Right) x 2 facing-direction (facing/non-facing) repeated-measures ANOVA.

Behaviour-only and TMS experiments

All procedures and analyses were pre-registered on aspredicted.org (https://aspredicted.org/4CZ_GGG). Deviations from the pre-registrations are indicated in the corresponding sections. The procedures were approved by the Research Ethics Committee of Bangor University's School of Psychology. Participants were community members of Bangor University and provided informed consent before participation. They were compensated with course credits, or a cash payment. Each participant only took part in one experiment.

Participants: Behaviour-only experiment. With this study, we sought to replicate the two-body inversion effect (2BIE) using stimuli, task and procedures from the original study that first reported that effect (Papeo et al., 2017). To this end, 25 participants were recruited (18 females, 7 males, mean age 20, SE = 1.3). This sample size matched Papeo et al. (2017) and allowed for achieving 80% power for an effect size of at least d = 0.58 on a two-tailed t-contrast. Two participants were excluded because their mean accuracy (1 participant) or response times (1 participant) were >2.5 above or below the group mean across conditions.

Participants: TMS experiment. Twenty-nine participants (16 females, 12 males, 1 other, mean age 24.34) took part in the TMS study. They were screened following the safety screening standard questionnaire for rTMS (Rossi et al., 2021). None of them reported a history of neurological, psychiatric, or other major medical disorders. Three participants were excluded from further analysis because their accuracy was 2.5 *SD*s below the group mean across conditions, yielding a final sample of 26. A sample size of 25 participants was pre-registered, to match the sample size of the above behaviour-only study, where we successfully oreplicated the 2BIE (see Results). However, to allow full counterbalancing of the stimulation site (participant starting with EBA/OPA stimulation) we tested one additional participant.

fMRI – Functional localisation of TMS sites. Each participant in the TMS study first completed two to four runs of a functional localizer task in the fMRI on a different date (~ 1 week before the TMS session). The task involved four conditions (human bodies without heads, unfamiliar faces, outdoor scenes, and chairs), each presented in four blocks of 18s in each run, interspersed with 5 fixation blocks of 16 s duration, for a total of 21 blocks per run. In each block, 24 images (selected randomly from a full set of 40) were presented, each for 300 ms, followed by a 450 ms blank interval. Twice during each block, an image was presented twice in a row. Participants were instructed to detect and report these repetitions by pressing a key.

Imaging data were acquired using a 3T Philips MRI scanner with a 32-channel SENSE phased-array head coil at the Bangor Imaging Centre in Bangor, Wales (UK). Functional data (T2* weighted, gradient echo sequence, echo time, 35ms; flip angle, 90°) were acquired with the following scanning parameters: repetition time 2s; 35 off-axial slices; voxel dimensions 3x3 mm; 3mm slice thickness; SENSE factor 2, phase encoding direction anterior-posterior. A high-resolution anatomical scan was also acquired (T1 weighted, 175 sagitally oriented slices; 1mm isotropic voxels; repetition time, 8.4 ms; echo time, 3.8 ms; flip angle 8°).

Functional MRI data were preprocessed and analyzed using SPM12 (Statistical Parametric mapping software; Wellcome Trust Centre for Neuroimaging, London, UK). The functional images were realigned, co-registered with the anatomical T1 image and spatially smoothed (6-mm FWHM Gaussian kernel). The resulting images were entered into a subject-specific general linear model with four conditions of interest corresponding to the four categories of visual stimuli. Estimates of the BOLD response in each voxel and category were derived by a general linear model including the boxcar functions of stimulation that were convolved with a standard hemodynamic response function. All analyses were performed in participant-native coordinates; for reporting purposes the coordinate of target sites were converted to standard MNI space (see **Figure 1C** and **Figure S7**).

For each participant, we localized the left hemisphere body and scene selective regions by contrasting the response to human bodies with that to the remaining three conditions and the response to scenes with that to the remaining three conditions, respectively. Each TMS target site (left hemisphere EBA; left OPA) was individually identified by selecting the peak activation for the relevant contrast, in the left lateral occipito-temporal cortex. The mean peak MNI coordinates (X, Y, Z, with SEM) were -45 (0.99), -73 (1.32), -2 (1.71) for the left EBA, and -32 (0.77), -84 (0.62), 17 (1.51) for the left OPA (see **table S1**, **Figure 1C** and **Figure S7** for individual coordinates).

TMS stimulation. A Magstim Rapid^2 (Magstim; Whitland, UK) with a 70mm figure-eight coil was used for the TMS. Stimulation intensity was set at 65% of the maximum stimulator output. This intensity corresponds to the average 120% of the resting motor threshold of Gandolfo & Downing (2019) using the same TMS equipment, and is similar to previous studies (Pitcher et al., 2007, 2008). Online TMS was delivered at 10Hz (2 pulses, 1 pulse every 100ms, for a total of 200 ms) with the handle pointing downward approximately at 45° from the middle sagittal axis of the participants' head (Candidi et al., 2008; Urgesi et al., 2004, 2007), adjusted to best project the pulse to the identified peak coordinate of each region and kept constant across stimulation sites. Such online stimulation protocol has been widely used to interfere with the ongoing processing of the preferred stimuli of category selective regions in occipito-temporal cortex (Pitcher et al., 2012; van Koningsbruggen et al., 2013).

TMS targeting was monitored with Brainsight 2.3.11 (Rogue Research), using individual structural and functional MRI images for each participant. The left EBA and left OPA were localized by overlaying individual activation maps from the localizer contrasts. The coil location was monitored online by the experimenter (Authors MG or EB) while participants

performed the task, and was maintained within 1mm of the defined point. The screen displaying the participants' task was out of view of the experimenters, rendering them blind to the condition on a trial-by-trial basis. To ensure temporal precision, the train of TMS pulses was triggered on each trial via a TTL pulse, initiated from a photosensor which detected a screen event (unseen by the participant) that co-occurred with the image onset on each trial.

Target hemisphere. Our pre-registration anticipated the stimulation of the right EBA, given that visual body-related effects consistently show right lateralisation (Gandolfo & Downing, 2019; Urgesi et al., 2007; van Koningsbruggen et al., 2013; Vangeneugden et al., 2014). However, an analysis on a pilot study involving 12 participants showed no modulation of the 2BIE, or any effect of TMS on task perfromance (see Supplemental Materials; **Figure S4, S5** and **S6**). Inparallel, we obtained the results of the fMRI re-analysis, which showed a strongly left-lateralized effect of facing *vs.* non-facing body dyads (see Results). Therefore, we reinvited the above 12 participants for another TMS study, in which everything was identical to the previous one except for the stimulation site: left EBA/OPA rather than right EBA/OPA. Eight out of 12 participants returned to the lab for this second study (COVID19-related disruptions caused the remaining participants to leave Bangor University before they could join the experimental session). The analysis of data from these 8 participants showed a significant Hemisphere x Site x Orientation x Facing Direction interaction when viewing human stimuli ($F(1,7) = 6.14$, $p = 0.042$, $\eta_p^2 = 0.47$, see supplemental materials for the full results). Thus, both our fMRI results and these preliminary TMS results pointed to the left (vs. right) hemispehere as being involved in the current effect. For this reason, and to avoid unnecessary brain stimulation, the remaining paricipants reported in the TMS study were only stimulated on the left ROIs. All the other procedures remained the same as described in the pre-registration. Data for the twelve participants on the right hemisphere are available on the OSF (OSF | Left EBA stimulation disrupts configural processing of face-to-face human dyads).

Stimuli. Stimuli included facing and non-facing human body dyads, pairs of facing and non-facing chairs, and visual masks, taken from Papeo et al. (2017). For each category, facing and non-facing stimuli involved the very same items, differing only for the relative positioning. Importantly, the distance between between bodies in facing and non-facing dyads was matched by keeping the center-center distance of each pair equally distant from the center of the display (1.8˚ of visual angle). Moreover, the distance between the two closest points of the two bodies was comparable for facing and non-facing dyads (mean distances for facing in pixels: 42.5 +/- 9.8 SD; mean distances for nonfacing in pixels: 40.3 +/- 12.2 SD; Mann-Whitney *U* test of the difference: $z = 0.44$, $p = 0.660$). A similar approach was implemented for creating pairs of chairs (60 facing and 60 non-facing), starting from six unique exemplars. Like body dyads, pairs of facing and non-facing chairs included the very same items at a matched distance (~2 degrees of viual angle), and thus only differed for the relative positioning (see Papeo et al., 2017 for details on stimuli). Visual masks consisted of high-contrast Mondrian arrays (11° x 10°) of grayscale circles of variable diameter (0.4°-1.8°). All stimuli were shown on a gray background. Images were presented on a 18 inch CRT monitor screen (1024x768 px, 60Hz refresh rate). The task was coded using Psychtoolbox (Brainard, 1997) running on GNU Octave (Eaton, 1997) on a Xubuntu Linux machine.

Task Procedure. Participants were seated on a chair in front of the monitor at a distance of ~50 cm from the screen in a dimly lit room. For each trial, they were instructed to report whether they saw humans or chairs. Each trial included the following sequential events: a grey screen (200 ms), a central fixation cross (5 jittered durations ranging between 1 and 2 seconds in intervals of 250 ms), the stimulus (upright/inverted facing/non-facing human dyad or pair of chairs) shown for 34 ms (2 screen refreshes at 60hz), and a visual mask shown for 300 ms. Participants were asked to respond “humans” or “chairs” as accurately and as quickly as possible, by pressing <f> or <j> on the keyboard. The key to response mapping was randomised across participants. Every 32 trials, participants were invited to take a break. Before starting, participants performed a practice block of 32 trials. The first 16 practice trials showed the stimuli for 250ms, so that participants could see the stimuli clearly and become familiar with them. In the second half of the practice block, the images were presented at the same speed as in the experiment (34 ms). Participants were offered the opportunity to perform an additional practice block, if needed. In the TMS version of the experiment, everyhitng was identical to the above, except that the experimenter (MG or EB) applied TMS pulses online, with the TMS coil placed on on the participant’s scalp.

Design. In the behaviour-only study, participants completed 256 trials divided in eight counterbalanced blocks of 32 trials (4 trials for each stimulus category, orientation, and facing direction presented in random order). During the TMS study, participants completed this task twice, once for each stimulation site. The site of first stimulation was counterbalanced across participants.

Analyses. Statistical significance was tested with factorial design ANOVAs and follow-up t-tests. Significance level was set at $p = 0.05$. In line with previous reports with this task we report analyses of Accuracy (% errors), computed for each condition. We performed a 2x2x2 within-subjects ANOVA with Stimulus (People/Chairs) x Orientation (Upright/inverted) x Facing Direction (Facing/non-facing) for the initial behaviour-only study. In the case of a significant interaction we compared the inversion effect (% errors for upright minus inverted stimuli) for facing *vs* non-facing conditions for each stimulus. In the TMS study, the design was the same, with the additional within-subjects factor of stimulation site (EBA/OPA). The interaction among all factors was further inspected with two separate ANOVAs, comparing the effects between the two types of stimuli, separately for each site, as well as two other ANOVAs comparing effects between the two stimulation sites, separately for each stimulus.

Where the absence of the effects was informative for the results, we added Bayes Factors as a complement to the null-hypothesis significance testing. We report BF10 calculated based on an uninformative standard Cauchy prior. Briefly, BF10 below 1 indicate that the null hypothesis is more likely, and values below 1/3 are generally taken as moderate, reliable evidence in favour of the null hypothesis (Jeffreys, 1961; Lee & Wagenmakers, 2013). For visualisation purposes, we calculated indexes subtracting the inversion effect for facing vs non-facing stimuli for each stimulation site. When such measure is positive, it indicates larger inversion effects for facing – vs – non-facing stimuli (Papeo et al., 2017).

Data pre-processing and analyses were conducted using R (Version 4.2.1) (R Core Team, 2022).

Data availability statement

The fMRI, behavioural and TMS data generated in this study, and the analyses scripts, are available at the OSF repository (https://osf.io/m9vp2/). The stimuli used in the three studies are available at https://osf.io/ur9jq/.

Acknowledgments

S. McKiernan for development of the custom photo-diode trigger, Sarah Salzgeber for task development and data collection in the behavioural experiment, Violette Munin for her help in the pre-processing and analysis of the fMRI data, and the Koldewyn lab for helpful discussions during lab meetings.

Funding

This project has received funding from the European Research Council under the European Union's Horizon 2020 research and innovation programme (ERC-2016-STG-716974: Becoming Social; awarded to K. Koldewyn), (ERC-2017-STG-758473 – THEMPO: awarded to L. Papeo), and the Marie Skłodowska-Curie ST-IF action (grant agreement No. 101033489 – memory-based percepts: awarded to M. Gandolfo).

Author Contributions

Marco Gandolfo: conceptualization, data curation, data visualization, formal analysis (behavioural and TMS), investigation, methodology, software, visualization, writing – original draft, writing review & editing.
Etienne Abassi: data curation, investigation, formal analysis (fMRI re-analysis), data curation, writing – review and editing, visualization.
Eva Balgova: investigation (TMS study), data curation, formal analysis (behavioural and TMS), writing – review and editing, visualisation
Paul E. Downing: conceptualization, methodology, software, writing – original draft, writing – review & editing.
Liuba Papeo: conceptualization, methodology, resources, writing – review & editing, supervision, funding acquisition.
Kami Koldewyn: conceptualization, methodology, writing – original draft, writing – review & editing, supervision, funding acquisition.

References

Abassi, E., & Papeo, L. (2020). The representation of two-body shapes in the human visual cortex. *Journal of Neuroscience*, *40*(4), 852–863. https://doi.org/10.1523/JNEUROSCI.1378-19.2019

Abassi, E., & Papeo, L. (2022). Behavioral and neural markers of visual configural processing in social scene perception. *NeuroImage*, 119506. https://doi.org/10.1016/j.neuroimage.2022.119506

Abassi, E., & Papeo, L. (2023). Category-selective encoding of social relationship in visual cortex. *In Prep.*

Adams, R. B., Ambady, N., Nakayama, K., & Shimojo, S. (2011). The Science of Social Vision. *The Science of Social Vision*, 1–504. https://doi.org/10.1093/ACPROF:OSO/9780195333176.001.0001

Adibpour, P., Hochmann, J.-R., & Papeo, L. (2021). Spatial Relations Trigger Visual Binding of People. *Journal of Cognitive Neuroscience*, *33*(7), 1–11. https://doi.org/10.1162/jocn_a_01724

Adolphs, R. (2001). The neurobiology of social cognition. *Current Opinion in Neurobiology,* 11(2), 231–239. https://doi.org/10.1016/S0959-4388(00)00202-6

Adolphs, R. (2009). The social brain: Neural basis of social knowledge. *Annual Review of Psychology*, *60*, 693–716. https://doi.org/10.1146/annurev.psych.60.110707.163514

Allison, T., Puce, A., Spencer, D. D., & McCarthy, G. (1999). Electrophysiological Studies of Human Face Perception. I: Potentials Generated in Occipitotemporal Cortex by Face and Non-face Stimuli. *Cerebral Cortex*, *9*(5), 415–430. https://doi.org/10.1093/CERCOR/9.5.415

Ashburner, J. (2007). A fast diffeomorphic image registration algorithm. *NeuroImage*, *38*(1), 95–113. https://doi.org/10.1016/j.neuroimage.2007.07.007

Belin, P., Bestelmeyer, P. E. G., Latinus, M., & Watson, R. (2011). Understanding Voice Perception. *British Journal of Psychology*, *102*(4), 711–725. https://doi.org/10.1111/J.2044-8295.2011.02041.X

Bellot, E., Abassi, E., & Papeo, L. (2021). Moving Toward versus Away from Another: How Body Motion Direction Changes the Representation of Bodies and Actions in the Visual Cortex. *Cerebral Cortex*, *31*(5), 2670–2685. https://doi.org/10.1093/cercor/bhaa382

Bracci, S., Letswaart, M., Peelen, M. V., & Cavina-Pratesi, C. (2010). Dissociable neural responses to hands and non-hand body parts in human left extrastriate visual cortex. *Journal of Neurophysiology*, *103*(6), 3389–3397. https://doi.org/10.1152/JN.00215.2010

Brainard, D. H. (1997). The Psychophysics Toolbox. *Spatial Vision*, *10*(4), 433–436. https://doi.org/10.1163/156856897X00357

Brothers, L. (1990). The social brain: a project for integrating primate behavior and neuropsychology in a new domain. *Concepts in Neuroscience*, *1*, 27–51.

Candidi, M., Urgesi, C., Ionta, S., & Aglioti, S. M. (2008). Virtual lesion of ventral premotor cortex impairs visual perception of biomechanically possible but not impossible actions. *Social Neuroscience*, *3*(3–4), 388–400. https://doi.org/10.1080/17470910701676269

Castelli, F., Happé, F., Frith, U., & Frith, C. (2000). Movement and Mind: A Functional Imaging Study of Perception and Interpretation of Complex Intentional Movement Patterns. *NeuroImage*, *12*(3), 314–325. https://doi.org/10.1006/NIMG.2000.0612

Centelles, L., Assaiante, C., Nazarian, B., Anton, J. L., & Schmitz, C. (2011). Recruitment of both the mirror and the mentalizing networks when observing social interactions depicted by point-lights: A neuroimaging study. *PLoS ONE*, *6*(1). https://doi.org/10.1371/journal.pone.0015749

Desikan, R. S., Ségonne, F., Fischl, B., Quinn, B. T., Dickerson, B. C., Blacker, D., Buckner, R. L., Dale, A. M., Maguire, R. P., Hyman, B. T., Albert, M. S., & Killiany, R. J. (2006). An automated labeling system for subdividing the human cerebral cortex on MRI scans into gyral based regions of interest. *NeuroImage*, *31*(3), 968–980. https://doi.org/10.1016/j.neuroimage.2006.01.021

Dilks, D. D., Julian, J. B., Paunov, A. M., & Kanwisher, N. (2013). The Occipital Place Area Is Causally and Selectively Involved in Scene Perception. *Journal of Neuroscience*, *33*(4), 1331–1336. https://doi.org/10.1523/JNEUROSCI.4081-12.2013

Downing, P. E., Jiang, Y., Shuman, M., & Kanwisher, N. (2001). A cortical area selective for visual processing of the human body. *Science (New York, N.Y.)*, *293*(5539), 2470–2473. https://doi.org/10.1126/science.1063414

Downing, P. E., & Peelen, M. V. (2011). The role of occipitotemporal body-selective regions in person perception. *Cognitive Neuroscience*, *2*(3–4), 186–203. https://doi.org/10.1080/17588928.2011.582945

Downing, P. E., & Peelen, M. V. (2016). Body selectivity in occipitotemporal cortex: Causal evidence. *Neuropsychologia*, *83*, 138–148. https://doi.org/10.1016/J.NEUROPSYCHOLOGIA.2015.05.033
Duchaine, B., & Yovel, G. (2015). A Revised Neural Framework for Face Processing. *Annual Review of Vision Science*, *1*(1), 393–416. https://doi.org/10.1146/ANNUREV-VISION-082114-035518
Eaton, J. W. (1997). *GNU Octave A high-level interactive language for numerical computations Edition 3 for Octave version 2.1.x*.
Friston, K. J., Ashburner, J., Kiebel, S., Nichols, T., & Penny, W. D. (2007). *Statistical parametric mapping : the analysis of funtional brain images*. Elsevier/Academic Press.
Gandolfo, M., & Downing, P. E. (2019). Causal Evidence for Expression of Perceptual Expectations in Category-Selective Extrastriate Regions. *Current Biology*, *29*(15), 2496-2500.e3. https://doi.org/10.1016/J.CUB.2019.06.024
Gandolfo, M., & Downing, P. E. (2020). Asymmetric visual representation of sex from human body shape. *Cognition*, *205*, 104436. https://doi.org/10.1016/J.COGNITION.2020.104436
Georgescu, A. L., Kuzmanovic, B., Santos, N. S., Tepest, R., Bente, G., Tittgemeyer, M., & Vogeley, K. (2014). Perceiving nonverbal behavior: Neural correlates of processing movement fluency and contingency in dyadic interactions. *Human Brain Mapping*, *35*(4), 1362–1378. https://doi.org/10.1002/hbm.22259
Gerlach, C., & Mogensen, E. (2023). The face inversion effect does not provide a pure measure of holistic face processing. *Behavior Research Methods*, *1*, 1–12. https://doi.org/10.3758/S13428-022-02054-5
Giese, M. A., & Poggio, T. (2003). Cognitive neuroscience: Neural mechanisms for the recognition of biological movements. *Nature Reviews Neuroscience*, *4*(3), 179–192. https://doi.org/10.1038/nrn1057
Griffin, J. W., & Oswald, F. (2022). A multilevel Bayesian meta-analysis of the body inversion effect: Evaluating controversies over headless and sexualized bodies. *Psychonomic Bulletin and Review*, *29*(5), 1558–1593. https://doi.org/10.3758/S13423-022-02067-3
Hu, Y., Baragchizadeh, A., & O'Toole, A. J. (2020). Integrating faces and bodies: Psychological and neural perspectives on whole person perception. *Neuroscience & Biobehavioral Reviews*, *112*, 472–486. https://doi.org/10.1016/J.NEUBIOREV.2020.02.021
Isik, L., Koldewyn, K., Beeler, D., & Kanwisher, N. (2017). Perceiving social interactions in the posterior superior temporal sulcus. *Proceedings of the National Academy of Sciences*, 201714471. https://doi.org/10.1073/pnas.1714471114
Jeffreys, H. (1961). *Theory of Probability. 3rd Edition, Clarendon Press, Oxford.* 470. https://global.oup.com/academic/product/theory-of-probability-9780198503682
Jenkinson, M., Beckmann, C. F., Behrens, T. E. J., Woolrich, M. W., & Smith, S. M. (2012). FSL. *NeuroImage*, *62*(2), 782–790. https://doi.org/10.1016/j.neuroimage.2011.09.015
Kaiser, D., & Peelen, M. V. (2018). Transformation from independent to integrative coding of multi-object arrangements in human visual cortex. *NeuroImage*, *169*, 334–341. https://doi.org/10.1016/j.neuroimage.2017.12.065
Kaiser, D., Quek, G. L., Cichy, R. M., & Peelen, M. V. (2019). Object Vision in a Structured World. In *Trends in Cognitive Sciences* (Vol. 23, Issue 8, pp. 672–685). Elsevier Ltd. https://doi.org/10.1016/j.tics.2019.04.013
Kanwisher, N., McDermott, J., & Chun, M. M. (1997). The fusiform face area: a module in human extrastriate cortex specialized for face perception. *The Journal of Neuroscience*, *17*(11), 4302–4311. https://doi.org/10.1523/jneurosci.17-11-04302.1997
Landsiedel, J., Daughters, K., Downing, P. E., & Koldewyn, K. (2022). The role of motion in the neural representation of social interactions in the posterior temporal cortex. *NeuroImage*, *262*, 119533. https://doi.org/10.1016/J.NEUROIMAGE.2022.119533
Lee, M. D., & Wagenmakers, E. J. (2013). Bayesian cognitive modeling: A practical course. *Bayesian Cognitive Modeling: A Practical Course*, 1–264. https://doi.org/10.1017/CBO9781139087759
Lee Masson, H., & Isik, L. (2021). Functional selectivity for social interaction perception in the human superior temporal sulcus during natural viewing. *NeuroImage*, *245*, 118741. https://doi.org/10.1016/J.NEUROIMAGE.2021.118741
Lingnau, A., & Downing, P. E. (2015). The lateral occipitotemporal cortex in action. *Trends in Cognitive Sciences*, *19*(5), 268–277. https://doi.org/10.1016/J.TICS.2015.03.006
Maurer, D., Le Grand, R., & Mondloch, C. J. (2002). The many faces of configural processing. *Trends in Cognitive Sciences*, *6*(6), 255–260. https://doi.org/10.1016/S1364-6613(02)01903-4

McCarthy, P. (2018). *FSLeyes*. https://doi.org/10.5281/ZENODO.1887737
Meteyard, L., & Holmes, N. (2018). TMS SMART – Scalp mapping of annoyance ratings and twitches caused by Transcranial Magnetic Stimulation. *Journal of Neuroscience Methods*, *299*, 34–44. https://doi.org/10.1016/J.JNEUMETH.2018.02.008
Papeo, L. (2020). Twos in human visual perception. *Cortex*, 132, 473-478. https://doi.org/10.1016/j.cortex.2020.06.005
Papeo, L., & Abassi, E. (2019). Seeing social events: The visual specialization for dyadic human–human interactions. *Journal of Experimental Psychology: Human Perception and Performance*, *45*(7), 877–888. https://doi.org/10.1037/xhp0000646
Papeo, L., Goupil, N., & Soto-Faraco, S. (2019). Visual Search for People Among People. *Psychological Science*, *30*(10), 1483–1496. https://doi.org/10.1177/0956797619867295
Papeo, L., Stein, T., & Soto-Faraco, S. (2017). The Two-Body Inversion Effect. *Psychological Science*, *28*(3), 369–379. https://doi.org/10.1177/0956797616685769
Peelen, M. V., & Downing, P. E. (2005). Selectivity for the human body in the fusiform gyrus. *Journal of Neurophysiology*, *93*(1), 603–608. https://doi.org/10.1152/jn.00513.2004
Peelen, M. V., & Downing, P. E. (2007). The neural basis of visual body perception. *Nature Reviews Neuroscience*, *8*(8), 636–648. https://doi.org/10.1038/nrn2195
Pitcher, D., Charles, L., Devlin, J. T., Walsh, V., & Duchaine, B. (2009). Triple Dissociation of Faces, Bodies, and Objects in Extrastriate Cortex. *Current Biology*, *19*(4), 319–324. https://doi.org/10.1016/J.CUB.2009.01.007
Pitcher, D., Garrido, L., Walsh, V., & Duchaine, B. C. (2008). Transcranial Magnetic Stimulation Disrupts the Perception and Embodiment of Facial Expressions. *Journal of Neuroscience*, *28*(36), 8929–8933. https://doi.org/10.1523/JNEUROSCI.1450-08.2008
Pitcher, D., Goldhaber, T., Duchaine, B., Walsh, V., & Kanwisher, N. (2012). Two Critical and Functionally Distinct Stages of Face and Body Perception. *Journal of Neuroscience*, *32*(45), 15877–15885. https://doi.org/10.1523/JNEUROSCI.2624-12.2012
Pitcher, D., & Ungerleider, L. G. (2021). Evidence for a Third Visual Pathway Specialized for Social Perception. *Trends in Cognitive Sciences*, *25*(2), 100–110. https://doi.org/10.1016/J.TICS.2020.11.006
Pitcher, D., Walsh, V., Yovel, G., & Duchaine, B. (2007). TMS Evidence for the Involvement of the Right Occipital Face Area in Early Face Processing. *Current Biology*, *17*(18), 1568–1573. https://doi.org/10.1016/J.CUB.2007.07.063
R Core Team. (2022). *R: A Language and Environment for Statistical Computing*. https://www.R-project.org/
Reed, C. L., Stone, V. E., Bozova, S., & Tanaka, J. (2003). The body-inversion effect. *Psychological Science*, *14*(4), 302–308. https://doi.org/10.1111/1467-9280.14431
Rezlescu, C., Wilmer, J. B., & Caramazza, A. (2017). The Inversion , Part-Whole , and Composite Effects Reflect Distinct Perceptual Mechanisms With Varied Relationships to Face Recognition. *Journal of Experimental Psychology: Human Perception and Performance, 43*(12), 1961–1973. https://doi.org/10.1037/xhp0000400
Robertson, L. C. (1995). Hemispheric specialization and cooperation in processing complex visual patterns. *Hemispheric Communication.* ISBN: 9781315789156
Rossi, S., Antal, A., Bestmann, S., Bikson, M., Brewer, C., Brockmöller, J., Carpenter, L. L., Cincotta, M., Chen, R., Daskalakis, J. D., Di Lazzaro, V., Fox, M. D., George, M. S., Gilbert, D., Kimiskidis, V. K., Koch, G., Ilmoniemi, R. J., Pascal Lefaucheur, J., Leocani, L., … Hallett, M. (2021). Safety and recommendations for TMS use in healthy subjects and patient populations, with updates on training, ethical and regulatory issues: Expert Guidelines. *Clinical Neurophysiology*, *132*(1), 269–306. https://doi.org/10.1016/J.CLINPH.2020.10.003
Sapey-Triomphe, L. A., Centelles, L., Roth, M., Fonlupt, P., Hénaff, M. A., Schmitz, C., & Assaiante, C. (2017). Deciphering human motion to discriminate social interactions: a developmental neuroimaging study. *Social Cognitive and Affective Neuroscience*, *12*(2), 340–351. https://doi.org/10.1093/SCAN/NSW117
Schwarzlose, R. F., Baker, C. I., & Kanwisher, N. (2005). *Separate Face and Body Selectivity on the Fusiform Gyrus*. *25*(47), 11055–11059. https://doi.org/10.1523/JNEUROSCI.2621-05.2005
Soares, J. M., Magalhães, R., Moreira, P. S., Sousa, A., Ganz, E., Sampaio, A., Alves, V., Marques, P., & Sousa, N. (2016). A Hitchhiker's Guide to Functional Magnetic Resonance Imaging. *Frontiers in Neuroscience*, *10*, 515. https://doi.org/10.3389/FNINS.2016.00515

Taylor, J. C., & Downing, P. E. (2011). Division of labor between lateral and ventral extrastriate representations of faces, bodies, and objects. *Journal of Cognitive Neuroscience*, *23*(12), 4122–4137. https://doi.org/10.1162/JOCN_A_00091

Taylor, J. C., Wiggett, A. J., & Downing, P. E. (2007). Functional MRI Analysis of Body and Body Part Representations in the Extrastriate and Fusiform Body Areas. *Journal of Neurophysiology*, *98*(3), 1626–1633. https://doi.org/10.1152/jn.00012.2007

Urgesi, C., Berlucchi, G., & Aglioti, S. M. (2004). Magnetic Stimulation of Extrastriate Body Area Impairs Visual Processing of Nonfacial Body Parts. *Current Biology*, *14*(23), 2130–2134. https://doi.org/10.1016/J.CUB.2004.11.031

Urgesi, C., Calvo-merino, B., Haggard, P., Aglioti, S. M., Scientifico, C., Medea, I. E., Friuli, P., Giulia, V., & Vito, I.-S. (2007). Transcranial Magnetic Stimulation Reveals Two Cortical Pathways for Visual Body Processing. *Journal of Neuroscience*, *27*(30), 8023–8030. https://doi.org/10.1523/JNEUROSCI.0789-07.2007

van Koningsbruggen, M. G., Peelen, M. V., & Downing, P. E. (2013). A Causal Role for the Extrastriate Body Area in Detecting People in Real-World Scenes. *Journal of Neuroscience*, *33*(16), 7003–7010. https://doi.org/10.1523/JNEUROSCI.2853-12.2013

Vangeneugden, J., Peelen, M. V., Tadin, D., & Battelli, L. (2014). Distinct Neural Mechanisms for Body Form and Body Motion Discriminations. *Journal of Neuroscience*, *34*(2), 574–585. https://doi.org/10.1523/JNEUROSCI.4032-13.2014

Walbrin, J., Downing, P., & Koldewyn, K. (2018). Neural responses to visually observed social interactions. *Neuropsychologia*, *112*, 31–39. https://doi.org/10.1016/j.neuropsychologia.2018.02.023

Walbrin, J., & Koldewyn, K. (2019). Dyadic interaction processing in the posterior temporal cortex. *NeuroImage*, *198*(April), 1–26. https://doi.org/10.1016/j.neuroimage.2019.05.027

Wischnewski, M., & Peelen, M. V. (2021). Causal evidence for a double dissociation between object- and scene-selective regions of visual cortex: a preregistered TMS replication study. *Journal of Neuroscience*, *41*(4), 751-756. https://doi.org/10.1523/JNEUROSCI.2162-20.2020

Yin, R. K., & Yin. (1969). Looking At Upside-Down Faces. *Journal of Experimental Psychology*, *81*(1), 141–145. https://doi.org/10.1037/h0027474